

Primljen / Received: 16.1.2021.  
Ispravljen / Corrected: 19.9.2021.  
Prihvaćen / Accepted: 20.10.2021.  
Dostupno online / Available online: 10.3.2023.

# Investigation of concrete slabs made with cement based mortars under impact loads

## Authors:



Assoc.Prof. **R. Tuğrul Erdem**, PhD. CE  
Manisa Celal Bayar, University Turkey  
Faculty of Civil Engineering  
[tugrul.erdem@cbu.edu.tr](mailto:tugrul.erdem@cbu.edu.tr)  
Corresponding author



**Murat Berberoğlu**, MSc. CE  
Manisa Celal Bayar, University Turkey  
Faculty of Civil Engineering  
[murat.berberoglu@cbu.edu.tr](mailto:murat.berberoglu@cbu.edu.tr)



Assoc.Prof. **Engin Gücüyen**, PhD. CE  
Manisa Celal Bayar, University Turkey  
Faculty of Civil Engineering  
[engin.gucuyen@cbu.edu.tr](mailto:engin.gucuyen@cbu.edu.tr)

Research Paper

**R. Tuğrul Erdem, Murat Berberoğlu, Engin Gücüyen**

## Investigation of concrete slabs made with cement based mortars under impact loads

As structural members can be subjected to impact loading during their service life, impact experiments are applied for various materials and objects by taking different methods into consideration. The effect of impact load on concrete slabs prepared with cement-based mortars is investigated in this study. A total of nine slab specimens measuring 500 x 500 x 50 mm are tested within the experimental program. Test specimens are prepared to provide different strength values and tested under impact load using the drop test setup. The impact resistance values of the specimens are determined based on the acceleration, impact load and displacement values, as obtained by measurement devices. In addition, crack distribution of the specimens is observed during impact tests. It has been noted that mortar types have a significant effect on the impact behaviour of the specimens. The finite element analysis is generated for each specimen to verify experimental results. Time histories of the acceleration, displacement and impact load values of the selected test specimens are compared. The relationship between experimental and numerical analysis results is presented, which reveals that the finite element procedure can be used in the evaluation of dynamic response of test specimens under the low velocity impact loading.

### Key words:

concrete slab, drop test setup, impact load, numerical analysis

Prethodno priopćenje

**R. Tuğrul Erdem, Murat Berberoğlu, Engin Gücüyen**

## Ponašanje betonskih ploča od cementnog morta pri udarnom opterećenju

Na konstrukcije tijekom njihove uporabe mogu djelovati razna udarna opterećenja pa se stoga provode različite metode ispitivanja materijala i konstrukcija udarnim opterećenjem. U ovom se radu istražuje utjecaj udarnog opterećenja na betonske ploče izvedene od cementnog morta. U okviru eksperimentalnog programa ispitano je ukupno devet uzoraka ploča dimenzija 500 x 500 x 50 mm. Pripremljeni uzorci različitih čvrstoća ispitani su metodom padajućeg tereta. Udarna čvrstoća uzoraka određena je na temelju mjerenih vrijednosti ubrzanja, udarnog opterećenja i pomaka. Osim toga, tijekom pokusa određen je i raspored pukotina koje nastaju nakon udarnog opterećenja. Ustanovljeno je da vrsta morta bitno utječe na udarnu čvrstoću uzoraka. Za svaki je uzorak provedena i analiza konačnim elemenatima radi provjere eksperimentalnih rezultata. Na odabranim su uzorcima uspoređene vrijednosti ubrzanja, pomaka i udarnog opterećenja. Prikazan je odnos između eksperimentalnih i numeričkih rezultata, a dobivene vrijednosti pokazuju da se metoda konačnih elemenata može primijeniti u ocjenjivanju dinamičkog odziva uzoraka podvrgnutih udarnom opterećenju male brzine.

### Ključne riječi:

betonska ploča, ispitivanje padajućim teretom, udarno opterećenje, numerička analiza

## 1. Introduction

Despite the brittleness property of conventional concrete, it is the most common building material in construction works. However, recent developments in materials science offer several advantages in construction technology. Grout mortars can be defined as cement based and self-consolidating materials. Besides, grout mortars can reach high strength values. They are used to cover areas due to their fluid, non-permeable and non-shrink properties. Short setting periods are provided due to presence of additive substances in the structure of mortars. Grout mortars can therefore be easily utilized in critical applications where rapid usage is needed.

The impact effect is basically defined as the changes in mechanical properties of objects at impact moment. The impact effect is investigated for several reasons. In fact, the effect of impact on various materials and structural members has recently been investigated by researchers in relation to vehicle collisions, falling rocks, projectile and missile strikes, sudden explosions, landslide, ship crashes with offshore structures, and crane accidents. The impact resistance of specimens is usually studied using well-designed drop test setups [1-8]. The performance of tests setups has been increased due to ASTM E 23 regulations that provide information about limits in impact tests [9].

It is not easy to provide for test conditions that would enable proper investigation of the behaviour of test specimens under the effect of impact loading. For this reason, numerical studies have recently been performed by researchers [10-17]. In addition, as the impact load is the least known type of load, the literature offers fewer studies about impact effect, compared to other types of static and dynamic loads. The investigation of test specimens under impact load is usually performed using appropriate equipment with test mechanism by dropping masses from certain drop height [18-23].

The aim of this study is to determine behaviour of test specimens subjected to sudden impact load. For this purpose, nine cement-based grout mortar slabs were prepared in laboratory. Various types of grout mortars were used to provide three distinct compression strength values. A test setup was developed for the experimental program. In this setup, various masses are dropped from several drop heights of up to 2500 mm.

While mass of the steel hammer that applies impact load on the specimens is 4.125 kg, the drop height is 600 mm. So, all specimens are tested under constant level of impact energy. These values are decided to follow crack patterns and damage distribution of test specimens during implementation of the experimental program. A high strength steel plate measuring 50x50x10 mm is used to prevent crushing from the point of impact loading, and to distribute the impact loading uniformly onto the specimens. Besides, a rubber layer is placed between the specimen and the steel plate to restrain stress localisation because of rough surface properties. In addition to test setup, measurement devices such as accelerometers, linear variable differential transformer (LVDT),

dynamic load cell, data logger systems, and optic photocells, are used to determine the acceleration, displacement, impact load, drop duration, and drop number. The experimental program is continued until failure damage situation is observed for all test specimens. So, damage development is monitored during the experimental program.

In the numerical analysis part of the study, the Abaqus finite elements software is utilized to obtain numerical solutions [24]. The explicit module of the software yields accurate results under incremental dynamic analysis. In addition, several material properties can be defined in this module. Acceleration, displacement and impact load values of test specimens are obtained after performing numerical analysis in the software. Afterwards, the acceleration-time, displacement-time, impact load-time and impact load-displacement graphs are comparatively presented. Finally, it is thought that this study will be useful in future studies investigating the impact behaviour of test specimens.

## 2. Experimental study

### 2.1. Test specimens and materials

In the experimental program implemented within the scope of the M.Sc. thesis [25], nine test specimens are produced in laboratory using three different types of cement-based grout mortars. While Specimens 1-3 are manufactured using the first type of grout mortar, Specimens 4-6 are manufactured using the second type, and Specimens 7-9 are manufactured using the third type. Test specimen dimensions are 500 x 500 x 50 mm. The behaviour of test specimens under impact load is investigated. While mass and drop height of the hammer are taken to be constant, strength values of the specimens are considered as experimental variables. Properties of mortar types used in the preparation of test specimens are given in Table 1.

**Table 1. Properties of mortar types**

Property	Type 1	Type 2	Type 3
Chemical content	Cement	Cement	Cement
Shape/colour	Dust/grey	Dust/grey	Dust/grey
Water amount [l] (for 25 kg bag)	2.27 – 3.50	2.75 – 3.25	2.5
Application temperature [°C]	0 - 25	5 - 30	2 – 35
Compression strength [N/mm <sup>2</sup> ]	30 - 35 (1 day)	≥ 60 (28 days)	≥ 90 (28 days)

A total of three sets are established to produce test specimens. For this purpose, various types of grout mortars are used. A homogenous mixture is prepared for each set and grout mortars are placed into moulds, as presented in Figure 1.



Figure 1. Grout mortars

Steel moulds measuring 40x40x120 mm are utilized in the determination of compression strength of test specimens. As shown in Figure 2, samples are taken from each test specimen. All test specimens and samples are kept in laboratory conditions during the necessary curing time.



Figure 2. Test specimen and samples

A total of 27 test samples belonging to 9 test specimens have been tested in the compression machine under axial load to define compressive strength values of test specimens. Finally, average compression strength values are calculated for test specimens by considering the results of cubic test samples. The values are given in Table 2.

Table 2. Compression strength values

Test specimen	Test sample	Compression strengths of test samples [N/mm <sup>2</sup> ]			Average compression strengths [N/mm <sup>2</sup> ]
S1	1. 2. 3	33.06	30.56	31.73	31.78
S2	4. 5. 6	30.45	29.70	31.69	30.61
S3	7. 8. 9	29.28	31.54	30.16	30.33
S4	10. 11. 12	66.59	64.18	65.91	65.56
S5	13. 14. 15	63.41	64.95	66.39	64.92
S6	16. 17. 18	66.74	65.19	67.98	66.64
S7	19. 20. 21	91.14	93.65	94.68	93.16
S8	22. 23. 24	93.41	91.55	92.62	92.53
S9	25. 26. 27	94.13	92.29	95.63	94.02

## 2.2. Test devices

Impact tests are performed using a test setup that is designed to investigate behaviour of test specimens under sudden impact load. According to literature [1-7], various researchers have used drop test setups for such experiments. In the test setup, the impact load is applied by a steel hammer. The drop height of the hammer can be varied by up to 2500 mm. Thus, different levels of impact energies can be applied on test specimens. The hammer measuring 200 x 200 mm is placed between two slides in the test setup. There is 200 mm distance between these slides in the test setup. The connection between the steel hammer and test setup is provided by four wheel-shaped members. These members are produced from castermid material to minimize friction effects during impact tests.

The base platform of the test setup, weighing almost 500 kg, is made of high strength steel plates. When placed on the ground, this platform measures 1000 x 1000 x 200 mm. Steel-made support devices are used to provide support to test specimens. The steel support devices measure 50 x 50 x 500 mm. These devices restrain horizontal and vertical movement in the across sides of test specimens.

The accelerometer, linear variable differential transformer (LVDT), dynamic load cell, data-logger, and optic photocells, are used in the experimental study as measurement devices. Schematic view of the test setup with measurement devices is presented in Figure 3.

The impact load is applied in the middle of the specimens. A high strength steel plate 10 mm in thickness, and a neoprene

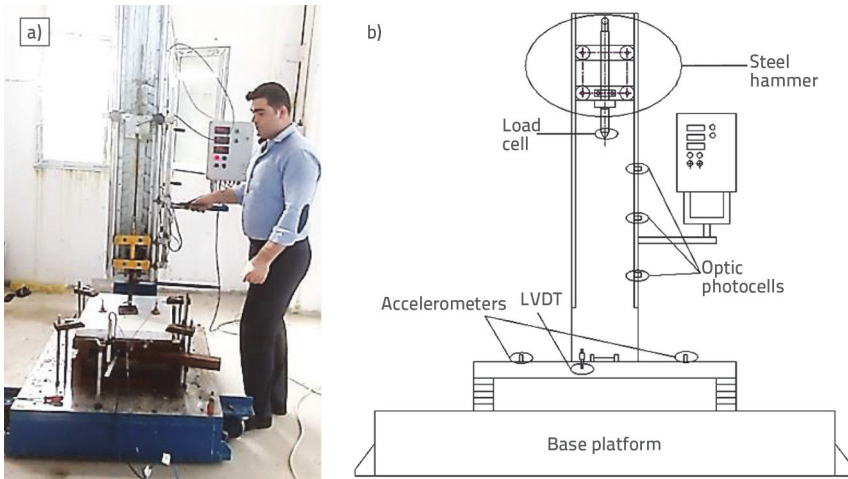


Figure 3. Test setup: a) Measuring devices; b) Schematic view

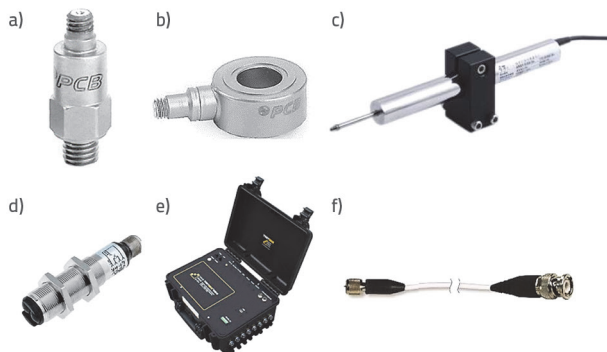


Figure 4. Test equipment in impact tests: a) Accelerometer; b) Load cell; c) LVDT; d) Optic photocell; e) Data logger; f) Connection cable

rubber layer 5 mm in thickness, are placed at the point of contact between the hammer and test specimen. Thus, the local fracture at the contact surface is prevented and the impact load is uniformly distributed on test specimens.

The ICP type piezoelectric accelerometers are symmetrically placed onto test specimens at 125 mm from the impact point. Acceleration values with vibrations are thus measured in a short span of time without any loss. In addition, the accelerometers have constant voltage sensitivity so that even

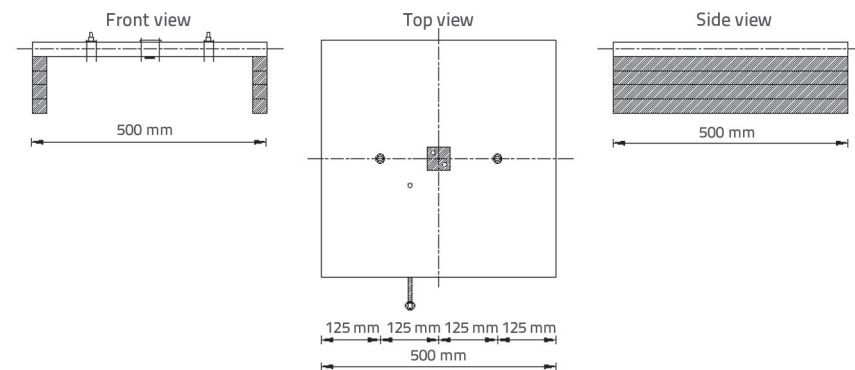


Figure 5. Test equipment on a test specimen

negative environmental conditions will not affect the signal quality of the accelerometers. These accelerometers have the measurement range of  $\pm 4905 \text{ m/s}^2$ , and their operating temperature varies between  $-18$  and  $+66^\circ\text{C}$ .

Displacement values are determined by LVDT for each drop of steel hammer. The mechanical movement of an object is changed into electrical signals by LVDT. The LVDT is fixed under test specimens around the impact point. The measurement range of LVDT is 50 mm, and the operating temperature varies between  $-18$  and  $+66^\circ\text{C}$ .

The impact load values are measured by the ICP typed dynamic load cell that is

placed at the edge part of the hammer. Load cell moves with steel hammer during each drop movement. Besides, it has the capacity to determine big signals with small waves in a short time. The measurement range of the load cell is up to 88.96 kN, and the operating temperature ranges from  $-54$  to  $+121^\circ\text{C}$ .

Optic photocells have two main tasks in this test setup. The first one is to enable the locking mechanism of the test setup. The impact load is thus applied on test specimens only once. Second load transfer from steel hammer to test specimen is prevented after the rebound movement of the hammer. The second task of the photocells is to measure the drop time and drop number. These values can be seen at the electronic screen of the test setup after each drop of steel hammer.

Special dynamic data logger systems are used during impact experiments, because sudden dynamic load is applied on test specimens. The measurement range, maximum sampling speed, ADC resolution, and power input values of the data-logger, are 138 dB, 16 kHz, 24 bit, and 12 vdc, respectively. The operating temperature of the data-logger varies between  $-20$  and  $+55^\circ\text{C}$ . The test equipment used in the experimental study is presented in Figure 4. Respective positions of test devices are shown in Figure 5.

### 3. Experimental results

Impact tests are performed after each specimen is placed in the test setup. The same amount of impact energy ( $4.125 \times 9.81 \times 0.6 = 24.28$  joule) is applied to test specimens and, at that, the mass and drop height values are constant. The steel hammer is lifted to the desired height and held at that level using a motorized mechanism with a magnetic clamping system. The hammer is then released and the impact load is applied on the specimens.

Table 3. Experimental results

Specimen No	Left acceleration [m/s <sup>2</sup> ]		Right acceleration [m/s <sup>2</sup> ]		Max. displacement [mm]	Max. impact load [N]
S1	- 813.64	736.30	- 794.41	723.72	8.90	18130.52
S2	- 693.24	741.88	- 736.68	677.56	8.52	18007.19
S3	- 730.50	690.02	- 685.93	719.34	9.04	17586.96
S4	- 980.60	938.97	- 962.56	935.17	7.07	21303.43
S5	- 958.80	1017.24	- 994.61	937.49	6.90	20976.14
S6	- 977.64	996.26	- 936.42	978.83	7.26	22045.69
S7	- 1363.03	1228.97	- 1213.58	1284.62	6.17	25243.09
S8	- 1176.24	1260.10	- 1163.42	1208.74	6.32	24946.20
S9	- 1255.95	1384.60	- 1249.04	1345.53	5.98	25534.37



Figure 6. Test specimen S5

Before impact experiments, test specimens are painted white so that development of cracks and damage can easily be observed. Support conditions of the specimens are provided during the experimental program. The test specimen S5 is shown as an example in Figure 6. Experimental program is continued until a failure damage situation is observed for each test specimen. In failure damage situation, maximum displacement value is measured by LVDT and test specimens can no longer resist impact load. In addition, some pieces of mortar separate from test specimens. Failure damages situations of all test specimens in the test setup are presented in Figure 7.

The values of acceleration, displacement, and impact load are measured during experimental program so as to determine general behaviour of test specimens under impact load [25]. The values of minimum and maximum acceleration, maximum displacement, and impact load, are given in Table 3. Because acceleration values

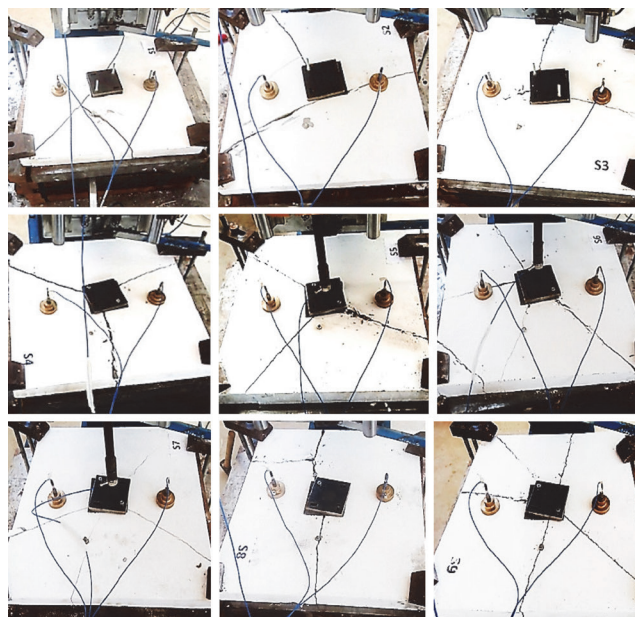


Figure 7. Failure of test specimens

are measured from two symmetrical accelerometers, left and right acceleration values are close to each other for each test specimen. Optic photocells that are placed along the drop height measure both drop numbers and drop durations. These values are shown on electronic screen of the test setup. Because the same amount of impact energy, reflecting the mass and drop height of the hammer, is utilized on the specimens, similar drop durations are obtained for test specimens. Average drop durations of test specimens differ from 374 to 385 milliseconds. On the other hand, failure drop numbers of the specimens differ from each other because of the compression strength values. Thus, the biggest drop numbers are obtained for specimens S7, S8, and S9 that were produced using the Type 3 mortar.

#### 4. Numerical analysis

In the numerical analysis part of the study, finite element models of the specimens are generated using the Abaqus software. The explicit module of Abaqus is capable of performing incremental

dynamic analysis under sudden impact load. Besides, many material models and failure characteristics are considered in the software. In recent times, researchers have been using the software to investigate behaviour of structural members under different load situations.

In the first step, test specimens, steel plate, and rubber layer, are modelled in the software. Three dimensional 10-node modified tetrahedron shaped (C3D10M) elements, widely utilized in impact simulations of structural members, are used for this purpose. The shape of the C3D10M elements is shown in Figure 8.

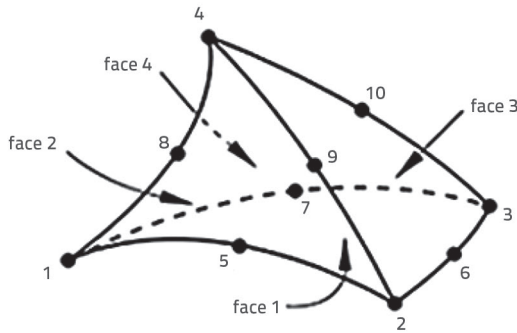


Figure 8. Failure of test specimens

Mesh sizes and time increments are important parameters that directly affect numerical results. These parameters directly influence the results of the analysis, and they are significant parts of the incremental dynamic analysis. The meshing operation was performed to separate finite elements models into smaller pieces. In addition, small time increments were used to obtain more accurate results. A study was performed to decide on the mesh size and time increments by considering the computational time. Finally, the mesh size of 20 mm, and time increments of  $2 \times 10^{-8}$  sec, were adopted in the analysis. 20893 nodes and 13075 elements were used for the specimens, 4614 nodes and 2897 elements were used for the hammer, and 273 nodes and 128 elements were used for rubber and plate.

Support conditions of the specimens are taken to be similar with the experimental study, and are assigned by considering the boundary conditions in horizontal, vertical and axial directions. Because the

problem is a free fall test, and impact load is applied by the steel hammer in vertical direction, only the vertical movement of the hammer is applied, and no external force, except the gravity force, is considered. The finite element model of Specimen 1, before and after mesh operation, is presented in Figure 9.

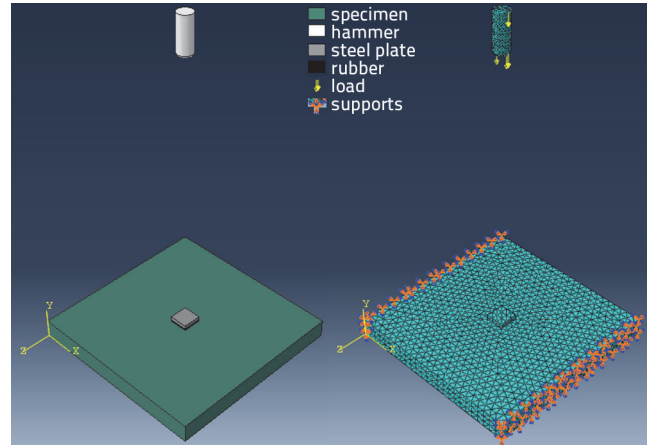


Figure 9. Finite element model of Specimen 1

As the friction effects can not be removed from the system completely, the coefficient of friction is defined as 0.02 for the contact surfaces in the software. The connection between the geometries is provided by interaction property of the software. For this purpose, the surface-to-surface contact property is used between the hammer and the specimen. While the surface of the hammer that applies the impact load is defined as master, the surface of the specimen is defined as slave in the software. Material properties of the slab, rubber layer, steel hammer, and plate are defined and assigned to the related geometries. The concrete damage plasticity model of the software is used to define the characteristics of the cement based concrete slabs. In this model, the behaviour is defined in both compression and tension regions, as presented in Figure 10. In the compression region, the path is linear until the initial yield value,  $\sigma_{co}$ . However, the response changes in the plastic because of stress hardening

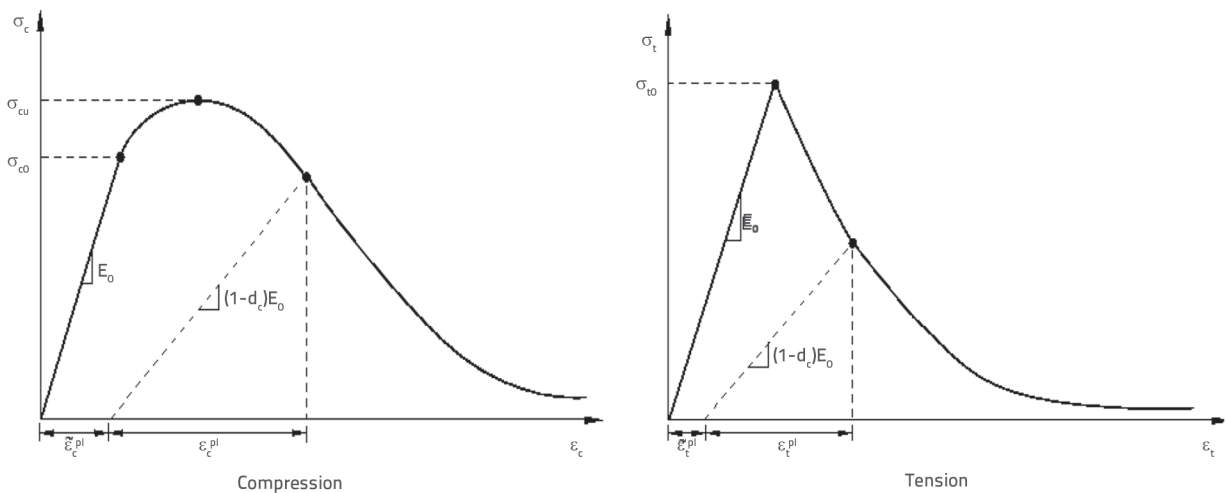


Figure 10. Material model for the slabs

followed by strain softening beyond the ultimate stress,  $\sigma_{cu}$ . In the tension region, the relationship is determined by linear elastic behaviour until the stress value of  $\sigma_{t0}$  is reached. After this point, the formation of micro cracks is generated by the response of softening stress-strain.

**Table 4. Material properties of slabs**

Property	Value
Poisson's ratio	0.20
Density [kg/m <sup>3</sup> ]	2400
$\Psi$	30
E	0.10
$\sigma_{b0}/\sigma_{c0}$	1.16
$K_c$	0.6667
m	0.0001

**Table 5. Properties of steel and rubber**

Property	Hammer and plate	Rubber
Poisson's ratio	0.30	0.45
Density [kg/m <sup>3</sup> ]	7850	1230
Young's modulus [MPa]	200000	22
Shear modulus [MPa]	76923	7.59
Bulk modulus [MPa]	166670	73.33

There are also other important parameters for plasticity such as the dilation angle, the flow potential eccentricity, the ratio of initial equibiaxial compressive yield stress to initial uniaxial

compressive yield stress, the coefficient determining the shape of the deviatoric cross-section, and viscosity. These parameters are used to define the yield surface function, potential flow, and material viscosity, as well as the compressive and tensile behaviour, and are symbolized by ( $\psi$ ), ( $e$ ), ( $\sigma_{b0}/\sigma_{c0}$ ), ( $K_c$ ) and ( $\mu$ ), respectively. In addition to these parameters, Young's modulus, Poisson's ratio, density, compressive strength, and tensile strength, are also defined in the software. The value of ultimate concrete strain ( $\epsilon_{cu}$ ) is taken to be 0.03. Furthermore, the equation ( $E_c=4700\sqrt{f_c}$ ) is used to calculate the Young's modulus while the equation ( $f_t=0.623\sqrt{f_c}$ ) is used to calculate the tensile strength values. The Young's modulus, compressive strength, and tensile strength, are separately defined for each specimen. Other material characteristics of the cement based concrete slabs are given in Table 4.

After completing material characteristics of slabs, properties of rubber layer, steel hammer and plate are also defined in the software. Linear elastic material models are utilized for this purpose. The values are presented in Table 5.

In the final step of the numerical study, the incremental dynamic analysis is performed for three slabs that have the biggest average compression strength value in each mortar type. So, the numerical analysis results of specimens 1, 6, and 9 are used in the verification of experimental results. The minimum and maximum acceleration, maximum displacement, and impact load values are obtained after numerical analysis in the software. The comparison of minimum and maximum acceleration values is given in Table 6, and maximum displacement and impact load values are comparatively presented in Table 7.

To reveal the relationship between experimental and numerical results, time histories of acceleration, displacement and impact

**Table 6. Comparison of acceleration results**

Specimen No	Acceleration [m/s <sup>2</sup> ]				Ratio*	Ratio**
	Experimental		Numerical			
S1	- 813.64	736.30	- 781.92	831.26	1.04	0.89
S6	- 977.64	996.26	- 945.38	918.67	1.03	1.08
S9	- 1255.95	1384.60	- 1187.26	1264.52	1.06	1.09
Prosjek					1.04	1.02

\*Ratio of experimental minimum acceleration values to numerical results  
\*\* Ratio of experimental maximum acceleration values to numerical results

**Table 7. Comparison of displacement and impact load results**

Specimen No	Displacement [mm]		Ratio***	Impact load [N]		Ratio****
	Experimental	Numerical		Experimental	Numerical	
S1	8.90	10.38	0.88	18130.52	20254.41	0.90
S6	7.26	8.16	0.90	22045.69	22964.37	0.96
S9	5.98	6.35	0.94	25534.37	24086.52	1.06
Prosjek			0.91	Prosjek		0.97

\*\*\*Ratio of experimental maximum displacement values to numerical results  
\*\*\*\* Ratio of experimental maximum impact load values to numerical results

load values are obtained for the selected slabs. In addition, load-displacement curves are formed by taking into consideration the same time intervals for impact load and displacement values.

Finally, the acceleration-time, displacement-time, impact load-time and impact load-displacement curves for the first drop of selected specimens are presented in figures 11-13.

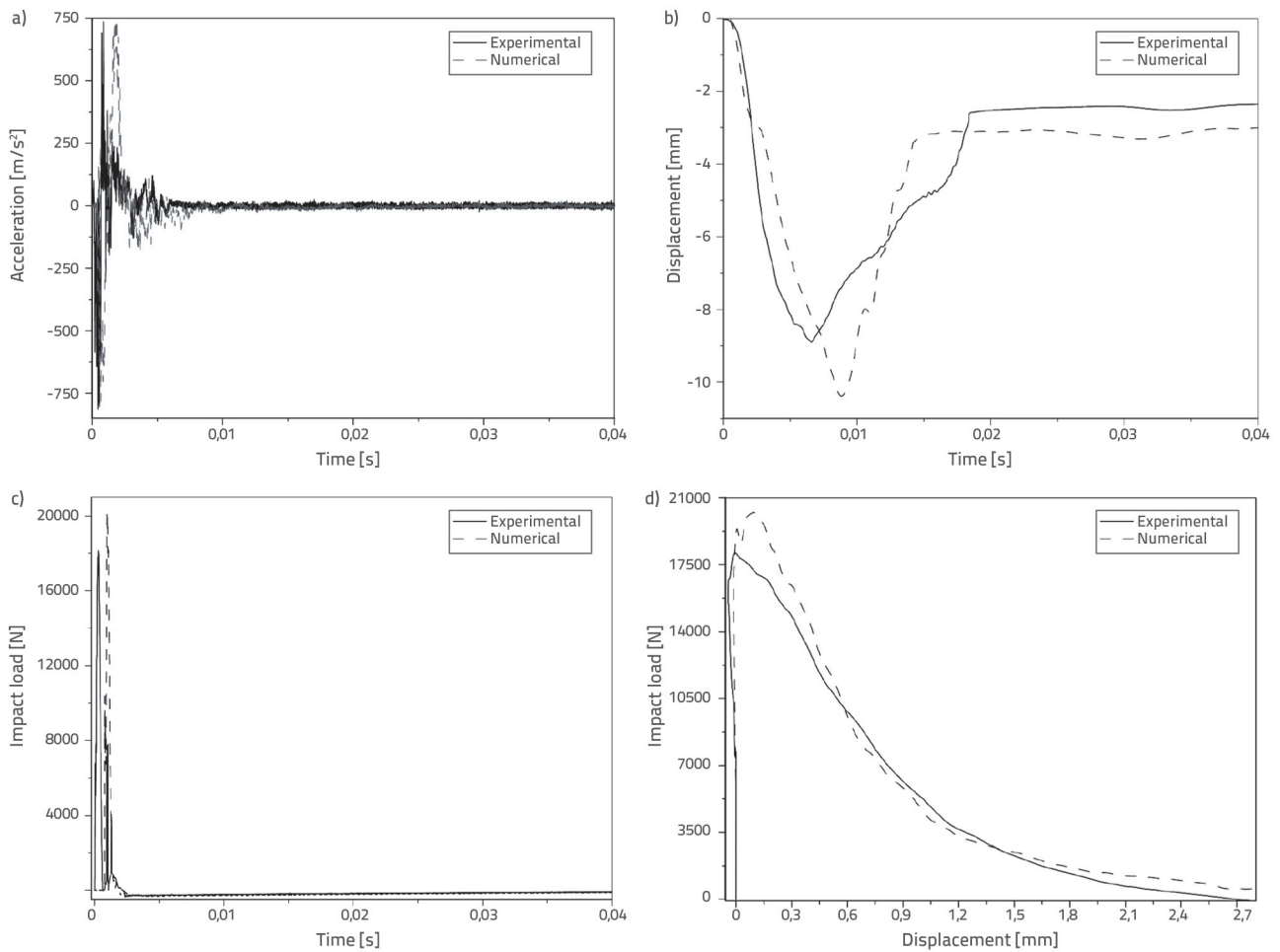


Figure 11. Graphs for S1 test specimen: a) Acceleration-time graph; b) Displacement-time graph; c) Impact load-time graph; d) Impact load-displacement graph

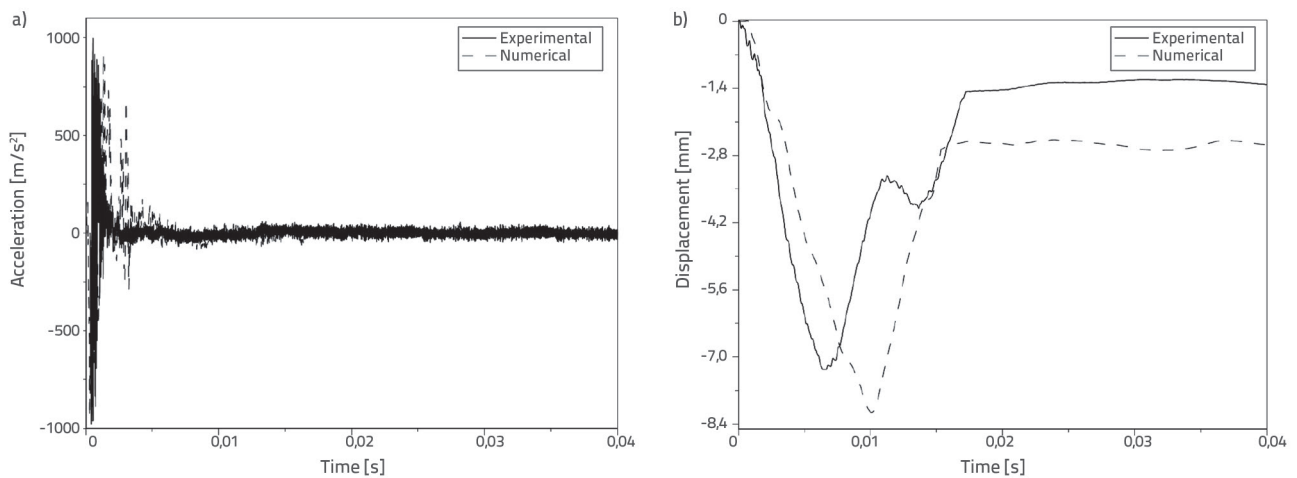


Figure 12. Graphs for test specimen S6: a) Acceleration-time graph; b) Displacement-time graph (prvi dio slike)

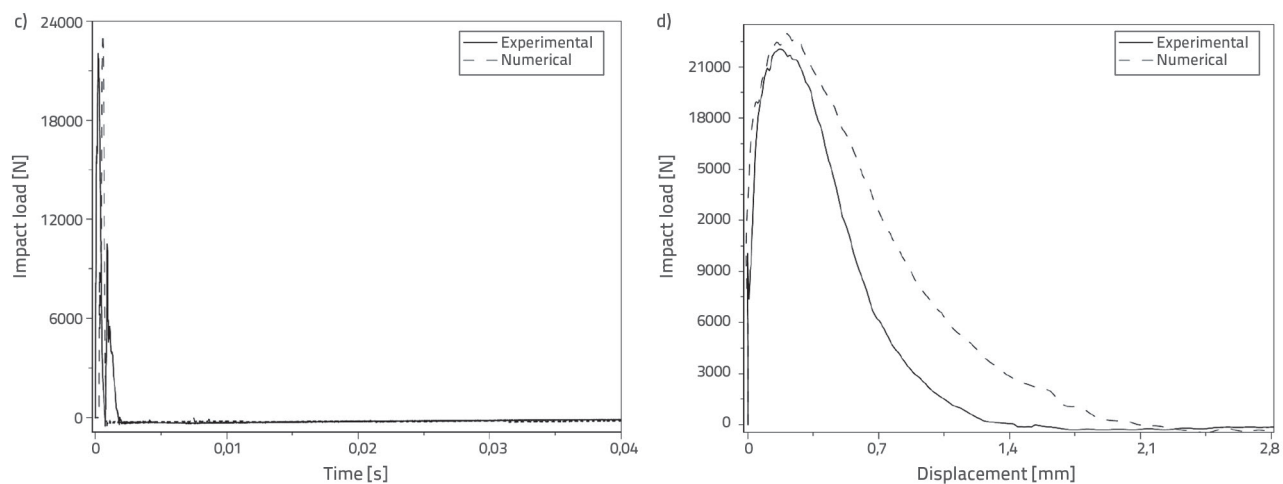


Figure 12. Graphs for test specimen S6: c) Impact load-time graph; d) Impact load-displacement graph (drugi dio slike)

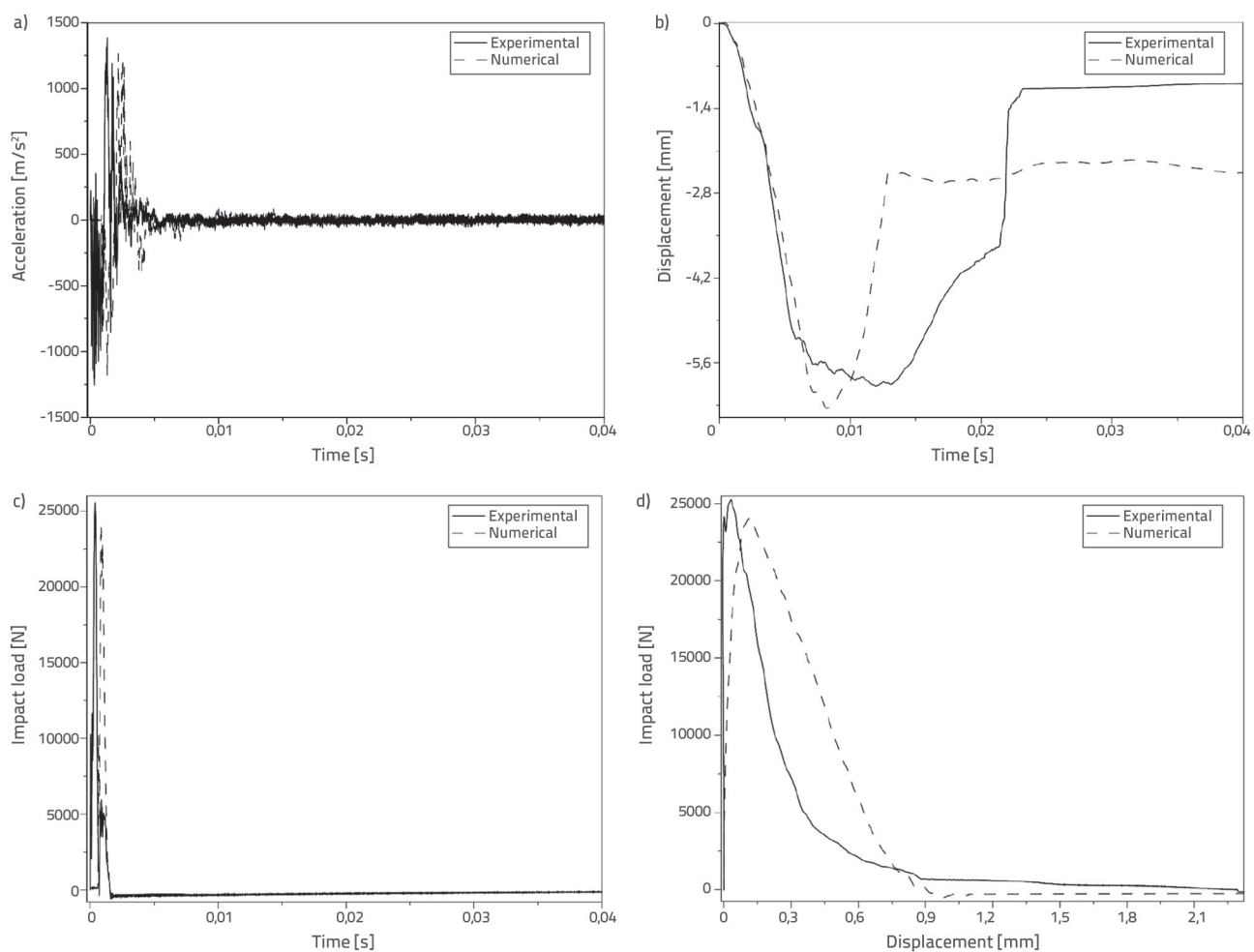


Figure 13. Graphs for test specimen S9: a) Acceleration-time graph; b) Displacement-time graph; c) Impact load-time graph; d) Impact load-displacement graph

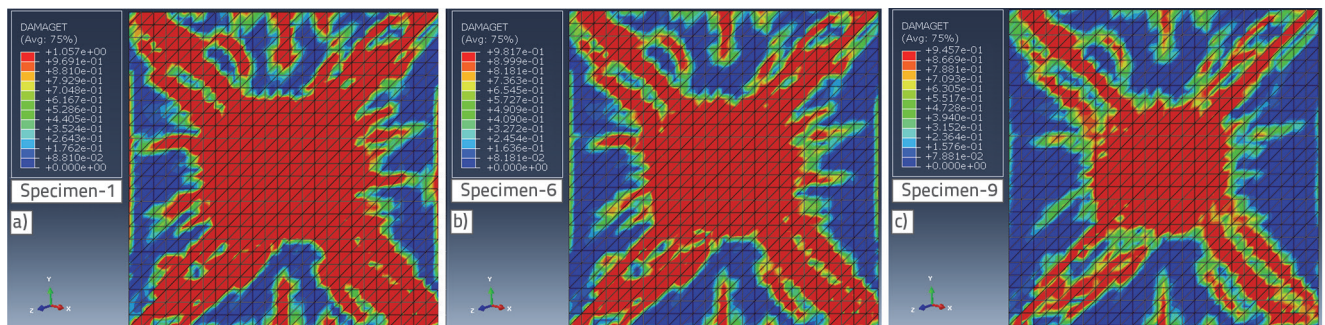


Figure 14. Damage patterns of the slabs: a) Numerical distributions for Specimen 1; b) Numerical distributions for Specimen 6; c) Numerical distributions for Specimen 9

Finally, the damage function of the software is used to obtain damage patterns of the specimens, as presented in Figure 14. This function gives consistent results in the determination of cracks on test specimens subjected to impact [26]. The damage is concentrated around mid-point of the slabs where the impact load is applied, and is then distributed to supports. It can also be seen that damage distribution is affected by rigidity due to compression strength value.

#### 4. Conclusion

The impact effect generally occurs when an object which has a definite velocity transiently strikes another object in stable position. Changes occur in the properties of materials or structural members due to sudden effects at impact moment. Main reasons for investigating the impact effect are basic incidents such as natural hazards, vehicle accidents, and explosions that may occur at the present time. Deformations and crack patterns due to high stresses that develop at impact moment are investigated by specially designed impact test setups.

The aim of this study is to determine dynamic response to sudden impact load of the slabs measuring 500 x 500 x 50 mm that are manufactured by using various types of grout mortars. A drop test setup is used to apply a constant level of impact energy on test specimens. Besides, measurement devices are utilized to determine the acceleration, displacement, impact load, and drop durations in the experimental program. The development of specimen damage is also observed during experimental study.

Experimental acceleration values reveal that results are greatly affected by rigidity of test specimens. Maximum acceleration values have been determined for test specimen S9, which has the highest compression strength value. The same tendency has also been

observed for the impact load values. The impact load values increase with an increase in compression strength. The biggest values are obtained for the specimens produced from the third type of mortar. When the displacement values are investigated in the experimental program, the biggest displacement value is measured for test specimen S1 that has the lowest compression strength. In addition, load-displacement curves are generated due to the combination of impact load and displacement values. The energy capacity values of test specimens are thus obtained. It can be seen that the behaviour becomes less ductile with an increase in rigidity of the specimens.

Drop durations and numbers are also followed during impact experiments. Since impact tests are performed for the same energy level of impact load, drop duration values are similar to each other. On the other hand, maximum drop numbers are obtained for test specimens S7, S8 and S9 whose compression strength values are bigger compared to other specimens.

The incremental dynamic analysis is performed in the numerical part of the study to investigate the behaviour of the selected slabs from each mortar type. Numerical analysis is generated so as to have the same conditions as the experimental study. The acceleration, displacement, impact load, and damage patterns of the slabs, are obtained using the software.

The analysis results are compared with experimental results, and a good correspondence has finally been established. Comparison of results reveals good compatibility between experimental and numerical values. However, small error rates are obtained between these results. Inner cracks, friction effects, and slight support movements during the experimental study, are considered to be the main reasons for these errors. Consequently, it is considered that the proposed finite element model could be an option for investigating the general impact behaviour of cement-based concrete slabs.

#### REFERENCES

- [1] Ranade, R., Li, V.C., Heard, V.F., Williams, B.A.: Impact resistance of high strength-high ductility concrete. *Cement and Concrete Research*, 98 (2017), pp. 24-35.
- [2] Yılmaz, T., Kırac, N., Anil, Ö., Erdem, R.T., Sezer, C.: Low velocity impact behaviour of two way rc slab strengthening with cfrp strips, *Construction and Building Materials*, 186 (2018), pp. 1046-1063.
- [3] Anil, Ö., Erdem, R.T., Tokgöz, M.N.: Investigation of lateral impact behavior of rc columns, *Computers and Concrete*, 12 (2018) 1, pp. 123-132.
- [4] Hering, M., Bracklow, F., Kühn, T., Curbach, M.: Impact experiments with reinforced concrete plates of different thicknesses, *Structural Concrete*, 21 (2020) 2, pp. 587-598.

- [5] Feng, S., Zhou, Y., Wang, Y., Lei, M.: Experimental research on the dynamic mechanical properties and damage characteristics of lightweight foamed concrete under impact loading, *International Journal of Impact Engineering*, 140 (2020), pp. 1-10.
- [6] Nataraja, M.C., Dhang, N., Gupta, A B.: Statistical variations in impact resistance of steel fiber-reinforced concrete subjected to drop weight test, *Cement and Concrete Research*, 29 (1999) 7, pp. 989-995.
- [7] Wang, B., Chen, Y., Fan, H., Jin, F.: Investigation of low-velocity impact behaviors of foamed concrete material, *Composites: Part B Engineering*, 162 (2019), pp. 491-499.
- [8] Xu, X., Ma, T., Ning, J.: Failure mechanism of reinforced concrete subjected to projectile impact loading, *Engineering Failure Analysis*, 96 (2019), pp. 468-483.
- [9] ASTM E23-00, Standard test methods for notched bar impact testing of metallic materials, ASTM International, West Conshohocken, PA, (2002).
- [10] Erdem, R.T., Gücüyen, E.: Non-linear analysis of reinforced concrete slabs under impact effect, *Građevinar*, 69 (2017) 6, pp. 479-487, <https://doi.org/10.14256/JCE.1557.2016>
- [11] Arros, J., Doumbalski, N.: Analysis of Aircraft Impact to Concrete Structures, *Nuclear Engineering and Design*, 237 (2007), pp.1241-1249.
- [12] Delhomme, F., Mommessin, M., Mougín, J.P., Perrotin, P.: Simulation of a Block Impacting a Reinforced Concrete Slab with a Finite Element Model and a Mass-Spring System, *Engineering Structures*, 29 (2007) 11, pp. 2844-2852.
- [13] Kostas, L.E., Riera, J.D., Iturrioz, I., Singh, R.L., Kant, T.: Analysis of Reinforced Concrete Plates Subjected to Impact Employing the Truss-Like Discrete Element Method, *Fatigue & Fracture of Engineering Materials & Structures*, 38 (2015) 3, pp. 276-289.
- [14] Mokhatar, S.N., Abdullah, R.: Computational Analysis of Reinforced Concrete Slabs Subjected to Impact Loads, *International Journal of Integrated Engineering*, 4 (2012) 2, pp. 70-76.
- [15] Tai, Y.S., Tang, C.C.: Numerical simulation: The Dynamic Behaviour of Reinforced Concrete Plates under Normal Impact, *Theoretical and Applied Fracture Mechanics*, 45 (2006), pp. 117-127.
- [16] Mokhatar, S.N., Abdullah, R., Kueh, A.B.H.: Computational impact responses of reinforced concrete slabs, *Computers and Concrete*, 12 (2013) 1, pp. 37-51.
- [17] Yankelevsky, D.Z.: Local response of concrete slabs to low velocity missile impact, *International Journal of Impact Engineering*, 19 (1997) 4, pp. 331-343.
- [18] Hrynyk, T.D., Vecchio, F.J.: Behavior of steel fiber-reinforced concrete slabs under impact load, *ACI Structural Journal*, 111 (2014) 5, pp. 1213-1224.
- [19] Radnic, J., Matešan, D., Grgic, N., Baloevic, G.: Impact testing of RC slabs strengthened with CFRP strips, *Composite Structures*, 121 (2015), pp. 90-103.
- [20] Xiao, Y., Li, B., Fujikake, K.: Behavior of reinforced concrete slabs under low velocity impact, *ACI Structural Journal*, 114 (2017) 3, pp. 643-650.
- [21] Zineddin, M., Krauthammer, T.: Dynamic response and behavior of reinforced concrete slabs under impact loading, *International Journal of Impact Engineering*, 34 (2007), pp. 1517-1534.
- [22] Zhang, M.H., Shim, V.P.W., Lu, G., Chew, C.W.: Resistance of high-strength concrete to projectile impact. *International Journal of Impact Engineering*, 31 (2005) 7, pp. 825-841.
- [23] Micallef, K., Sagasetta, J., Ruiz, M.F., Muttoni, A.: Assessing punching shear failure in reinforced concrete flat slabs subjected to localised impact loading, *International Journal of Impact Engineering*, 71 (2014), pp. 17-33.
- [24] ABAQUS User's Manual, Version 6.12, SIMULIA, Dassault Systèmes Simulia Corp., 2015.
- [25] Berberoğlu, M.: Experimental investigation of concrete slabs produced with cement based mortars under dynamic loads, M.Sc. Thesis, Manisa Celal Bayar University, 2019.
- [26] Yılmaz, T., Kırac, N., Anil, Ö., Erdem, R.T., Kaçaran, G.: Experimental Investigation of impact behaviour of RC Slab with different reinforcement ratios, *KSCE Journal of Civil Engineering*, 24 (2020) 1, pp. 241-254.